

J. Higgins and D. Keller

# A Compact Frozen Spin Refrigerator Design

Received: date / Accepted: date

**Abstract** A dilution refrigerator design is proposed that could be used as an insert to a pre-existing Oxford Instruments 1 K  $^4\text{He}$  evaporation refrigerator with a 5 T magnet. This insert is designed such that all dilution components fit within the geometric constraints presented by the Oxford cryostat. This system will be used in frozen spin studies where the sample material is polarized using dynamic nuclear polarization and then cooled to well below 100 mK. The polarization can be monitored using a continuous wave nuclear magnetic resonance coil coupled to the material during the polarization process and under frozen spin mode. The dynamic polarization and measurement process sets the scale for the expected heat load of this cryostat so design characteristics are specific to the system's thermal requirements.

**Keywords** Frozen Spin · Dilution Refrigerator · Dynamic Nuclear Polarization · Nuclear Magnetic Resonance

**PACS** 76.60.-k · 77.22.Ej

---

## 1 Introduction

The polarized solid state target [1] has been an integral part of spin dependent nuclear and particle physics experiments over the last 50 years. A polarized target system cools ( $T \leq 1\text{K}$ ) a polarizable material while in a homogeneous high magnetic field (2.5-5 T). Photoproduction scattering experiments typically use a  $^3\text{He}/^4\text{He}$  dilution refrigerator so that the desired target ensemble helicity can be held in a frozen-spin state ( $< 100\text{ mK}$ ) after the polarization enhancement from dynamic nuclear polarization (DNP). For high intensity ( $\sim 100\text{ nA}$ ) electron or proton beam scattering experiments a  $^4\text{He}$  evaporation refrigerator is required in combination with

a powerful pumping system. For frozen spin targets designed for beam interaction [2] a material such as irradiated  $\text{NH}_3$  or TEMPO-doped butanol can be dynamically polarized to over 90% at 5 T and 200-300 mK. A beam of photons or low intensity ( $10^7$  particles/sec) charge particles can be put on the target at a frozen-spin temperature of approximately 30 mK with the polarization maintained by a thin, superconducting coil (0.5 T) inside the target cryostat. Such a system allows for a large kinematic coverage by relying on this small holding coil, allowing the polarizing magnet to be removed. In the frozen-spin mode, spin-lattice relaxation times as high as 4000 hours have been observed implying very slow degradation of polarization over time.

We propose a design that is optimized only for test lab use and will not be used in scattering experiments. This system should be capable of polarization of a sample using dynamic nuclear polarization where the polarized sample is measured using continuous wave nuclear magnetic resonance (CW-NMR). The system must be thermally equipped to handle solid-state RF experiments and should be loadable with frozen solid target materials in the sample holder (mixing chamber). The dilution unit will fit into a pre-existing Oxford Instruments evaporation refrigerator-magnet combination such that the system will allow quick interchange between a high power evaporation refrigerator system and a low power low temperature system.

The present work is an investigation into the geometric constraints (the Oxford Cryostat), the systems thermal requirements, the actual design of the dilution insert, and some simulations and discussion of expected performance.

---

## 2 The Oxford Cryostat

The geometric constraints of the new dilution insert are defined by the limited space in the pre-existing cryostat and magnet. The magnet is an Oxford Instruments 8 T

---

Contact Author: D. Keller  
University of Virginia, Charlottesville, Virginia 22901  
Tel.: 434-243-9955  
E-mail: dustin@jlab.org

NbTi superconducting solenoid with a bucking cancellation coil. The magnet though capable of 8 T is operated at 5 T during DNP. The magnet consists of a coil which runs at 83.80 A at 4.2 K with a field homogeneity of  $\pm 0.001\%$ . The clear bore diameter is 77.5 mm with a current decay in persistent mode of less than  $1 \times 10^{-5}$  per hour. The magnet dewar holds approximately 40 L of liquid helium which is insulated with an inner-vacuum layer, a liquid nitrogen layer, and an external vacuum layer. The inner and outer vacuum layers are connected and continuously pumped during operation down to  $\sim 10^{-6}$  Torr using a turbo pump system. There is also a jumper-transfer line that connects the 40 L magnet dewar to the high cooling power evaporation refrigerator. This jumper is a vacuum insulated line that is used to transfer liquid helium into the evaporation refrigerator separator can.

The high cooling power evaporation refrigerator consists of a set of upper heat exchangers that are cooled when vapor from the separator is pumped through, using a helium compressor pump. Liquid comes into the separator via the jumper-transfer line from the liquid helium in the magnet. The liquid is pumped from the transfer line into the bottom of the separator can and up over the central sintered plate inside. A liquid reservoir at  $\sim 2.5$  K builds up in the separator and is used to feed the lower heat exchangers. The run valve can be opened to control the liquid helium flow from the separator down through the lower heat exchangers and into the main helium evaporator. Below the lower heat exchangers is the cold helium reservoir which is simply a helium space made from the refrigerator shell. This whole shell is connected to a high power pump stack to pump on the liquid helium volume creating a high degree of evaporation while passing the cold helium vapor over the lower and then upper heat exchangers to optimize cooling and functionality of the refrigerator. An example of a pump stack would be a mechanical backing pump, and then a  $350 \text{ m}^3/\text{hour}$  and then a  $1000 \text{ m}^3/\text{hour}$  ( $\sim 1 \text{ W}$  of cooling power with this system), but the pumping system can vary depending on the goals of the project.

This Oxford system has a KF-50 mouth opening on top where the material insert goes. The insert should be of the appropriate length and design to hold the sample material below the lower heat exchanges and in the center of the homogeneous field region. There is a central opening in the heat exchangers and the separator can of 50 mm in diameter, so that the insert can sit in the center of the cryostat. This system is fitted with a manometer connected to the evaporator pump-out that reads the helium vapor pressure. This is the most accurate temperature measurement of the cold helium reservoir in the evaporation region. Other sensors are fitted to various parts of the refrigerator to monitor operation of the cryostat. A schematic of the Oxford Instruments system is shown in Fig. 1.

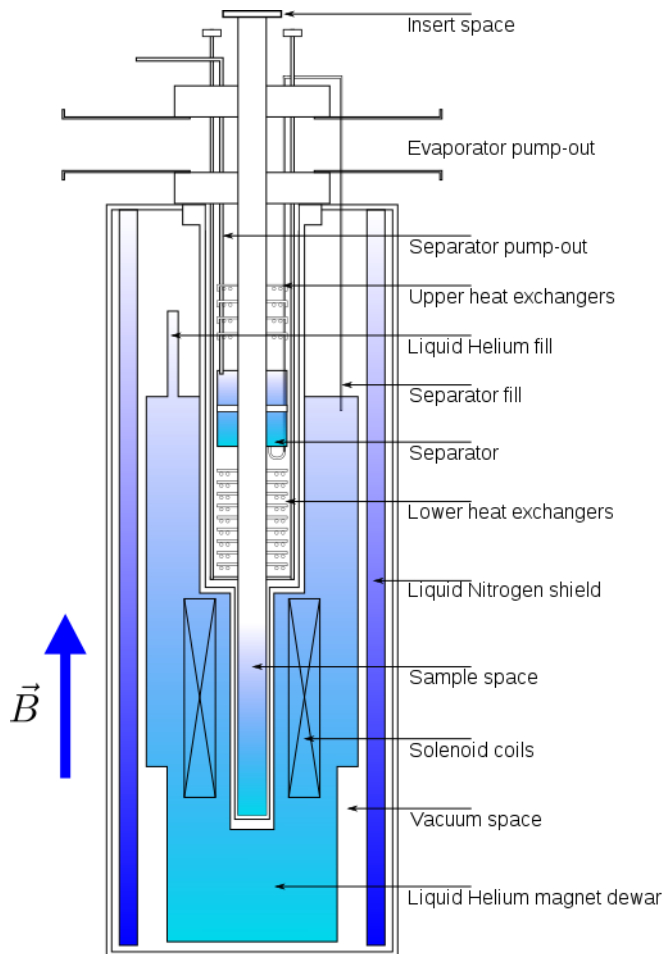


**Fig. 1** The Oxford Instruments original cryostat. This diagram indicates the starting evaporation refrigerator and superconducting solenoid that the dilution unit will fit into.

### 3 Goals and Thermal Requirements

The goals of the design for the dilution insert are such that the mixing chamber and material sample can be held around 50 mK. The diameter of the insert should be approximately 4 cm, and the top of the dilution unit has to reside underneath the liquid level within the cryostat, allowing a total length of 150 cm. Because this is a DNP system a microwave guide to deliver the 140 GHz polarizing microwaves must pass through the central line of the insert to irradiate the mixing chamber area. The microwave generator is an extended interaction oscillator (EIO) tube which connects to a D-band rectangular waveguide which bends at 90 degrees and then passes into a circular waveguide delivering the microwaves through the length of the refrigerator to the sample. Though the microwave system is capable of delivering nearly 1 W of microwave power on the sample this can be attenuated to a more manageable 50 mW. The polarization of the material takes place at a much higher temperature ( $\sim 1$  K) so this is not a heat load that

we concern ourselves with in regards to the operation of the dilution unit. However, it is necessary to make sure the waveguide does not create a heat leak down to the mixing chamber area.

The main operational heat load is from the CW-NMR system. This does not touch the sample but is inductively coupled to the material and does produce heat through radiofrequency (RF) irradiation of the sample in the tens of  $\mu\text{W}$  range if configured to run with low RF power. The RF induces nuclear spin flips during polarization measurements, however the CW-NMR system used is designed to be a non-destructive measurement by running as a low constant current Q-meter which works as part of a phase sensitive circuit which responds to the changes of the impedance in the NMR coil [3]. The RF susceptibility of the material is inductively coupled to the NMR coil as part of a series LCR circuit, tuned to the Larmor frequency of the nuclei being probed. This measurement system is expected to get better than 3% relative uncertainty in polarization during DNP [4]. The best way to deal with the heat load produced by the CW-NMR is to take infrequent polarization measurement, giving the cryogenic flows time to recover.

The novelty of mating a dilution unit and the Oxford cryostat is that the 1 K evaporation refrigerator of the Oxford system will be used as the condenser to the dilution insert. This is done by having the incoming  $^3\text{He}$ - $^4\text{He}$  gas mixture coming into the evaporation refrigerator already running so that the gas is pre-cooled. The insert will be constructed to regulate the temperature of this incoming gas by then passing down the separator region making thermal contact with this area and further condensing. Finally the gas is channeled through the cold helium reservoir and the 1 K plate where the main  $^4\text{He}$  evaporation takes place. At this stage the 1 K helium has a two fold function in that it works as the  $^3\text{He}$ - $^4\text{He}$  gas condenser and a 1 K insulation layer around the dilution unit making a cryogenic thermal shield.

#### 4 Design of the Dilution Insert

In this design the entire dilution insert, shown in Fig. 2, is approximately 1.5 m in length. From the top of the insert down approximately 60 cm is the location of the separator inside the Oxford cryostat. This region of the evaporation refrigerator will be in close proximity to the copper separator cylinder on the insert design. This is meant to be a thermal barrier in both the refrigerator and the insert and is thermally regulated at around 2.5 K. The progression of the temperature gradient in the insert will be similar to the Oxford cryostat until the 1 K region. The dilution unit is expected to have a total weight of about 1 kg, which must be supported by the tensile strength of the insert frame. Below the separator cylinder, there is 50 cm for the cold helium reservoir, the lower 26 cm of which is dedicated to the dilution unit.

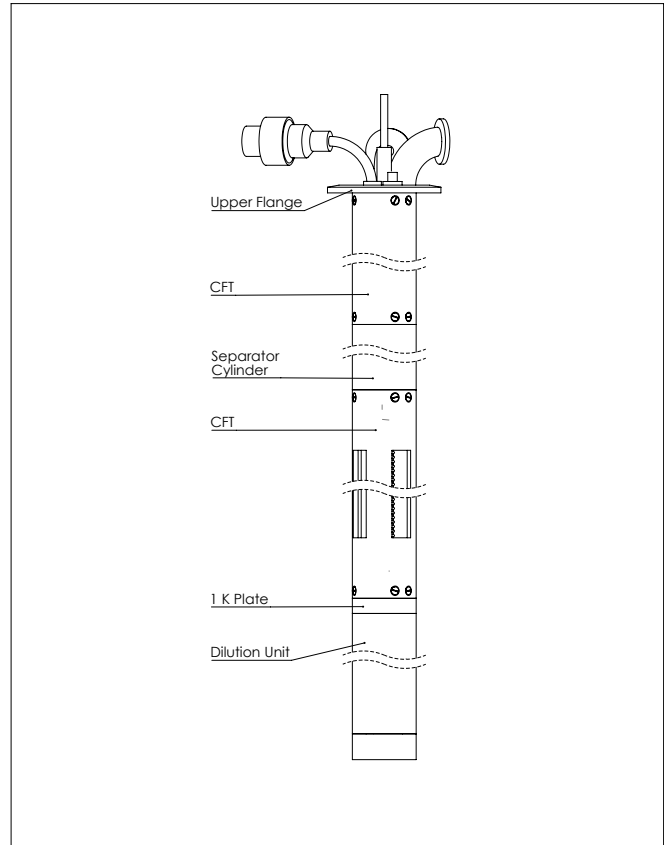


**Fig. 2** The insert proposed in this paper. It is inserted with the dilution unit first into the Oxford cryostat.

Between the dilution unit and the separator is a heat exchanger to help pre-cool the  $^3\text{He}$  as it is pumped towards the dilution unit before reaching the condenser. This pre-cooling heat exchanger ensures an adequate condensing rate of the gaseous  $^3\text{He}$  when first entering the refrigerator. The design of the non-dilution components are discussed in Sec. 4.1, and the dilution unit is discussed in Sec. 4.2.

It should be noted that the steel used in the design is 316 L stainless steel (unless otherwise specified for specific components). This particular steel has a low magnetic susceptibility and does not interact with the magnetic field generated by the superconducting solenoid.

From Fig. 2 it should be clear that the system is inserted with the dilution unit first into the Oxford cryostat. The upper flange supports the structure and can hold the rest of the insert's weight. This flange hermetically seals with a KF-50 O-ring and vacuum clamp onto the Oxford cryostat mouth. Carbon fiber tubing (CFT) mechanically connects the flange to the separator cylinder and the dilution unit.

#### 4.1 Upper Dilution refrigerator

The upper flange also supplies the necessary feed through to the inner refrigerator. Through this flange the NMR line, microwave line, inner vacuum line,  $^3\text{He}$  in and out lines, as well as a line for electronics all pass to the refrigerator.

Below the insert separator cylinder and the liquid level of the  $^4\text{He}$  reservoir is the 1 K plate, acting as a thermal barrier between the cooler dilution components below and the warmer pre-cooling components above. The CFT mechanically connects the separator cylinder to the upper flange, as well as the 1 K plate to the cylinder. Within this tubing runs all major lines down to the dilution unit. These major lines are anchored to the separator, the 1K plate, and then the dilution unit still to minimize heat transfer down to cooler regions of the system.

##### 4.1.1 Upper Flange

The upper flange will be made of stainless steel, 7.5 cm in diameter and 5 mm in thickness. The area on this flange is used conservatively in order for all components to fit and remain functional (Fig. 3).

On the bottom side of the upper flange (Fig. 4) is a 5.2 cm outer-diameter (OD) groove in which the 2 mm thick KF-40 O-ring will sit to make the hermetic seal. Also on the bottom is a 3.88 cm OD metal lip with six M3-threaded holes. Fitted over this lip is a carbon-fiber tube (CFT) that also has six M3-sized sunken screw holes so that machine screws of the same size and type may secure the CFT to the upper flange.

Both the  $^3\text{He}$  out line and vacuum line connect to their respective pumping systems with a KF 25 vacuum clamp. The  $^3\text{He}$  in line connects to a swagelok VCR metal fitting from the outside, and reduces in OD from 12 mm to 1.6 mm through the flange on the inside. The  $^3\text{He}$  out line reduces in OD from 19 mm to 9.6 mm, and the vacuum line and microwave line remain 7.5 mm and 4.75 mm, respectively.

##### 4.1.2 Cylinder/1 K Plate

A CFT connects to both the upper and lower portion of the separator cylinder in a similar fashion as the upper flange (see Fig. 5). Each line through the cylinder remains in a similar location as the upper flange.

The CFT below the separator cylinder has open channels so that the 1 K  $^4\text{He}$  from the evaporator will submerge the components. In this section, the  $^3\text{He}$  in line will spiral around the microwave line at the center as it descends to the 1 K plate, over a total length of 2.5 m, maximizing the pre-cooling. The CFT below the separator also connects to the top of the 1 K plate. Fig. 6 shows the features between the separator cylinder and the 1 K plate.

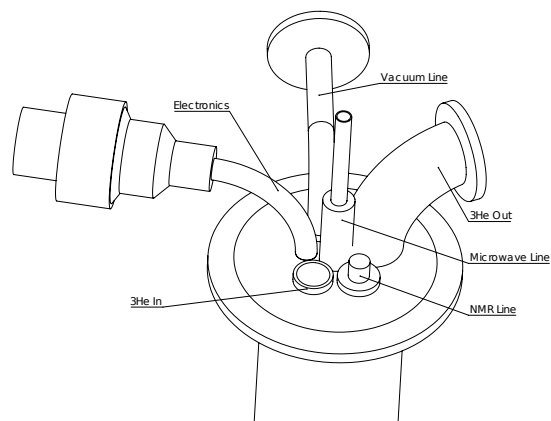


**Fig. 3** Top-angle view of the upper flange. This view shows the various components that run through the upper flange.

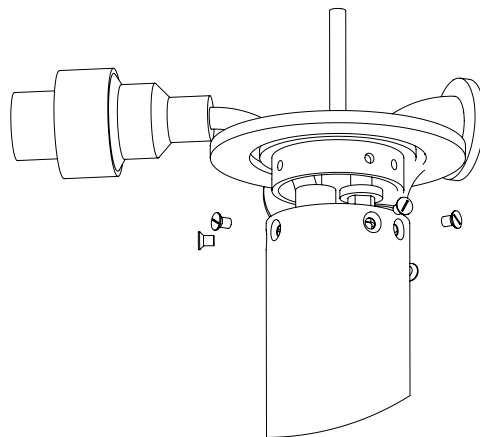


**Fig. 4** In this view, components are magnified to show how the insert is assembled. The CFT fits over a lip on the upper flange. Sunken M3-sized machine screws are connected through the holes on the CFT to the threaded holes of the upper flange, securing both components in place.

#### 4.2 Dilution Unit

Below the 1K plate are the dilution components of the insert. In Fig. 7 and 8 the dilution unit is shown with certain components removed in order to reveal a more comprehensive assembly. Shown in Fig. 7 is the 1 K Plate, the graphite connection between the 1 K and the still, the main heat exchanger, and the mixing chamber. As can be seen, the main heat exchanger spirals around the microwave line and NMR line that penetrates down the middle of the insert, terminating just above the mixing chamber. Shown in Fig. 8 is the graphite support between still and mixing chamber. The support between the still and mixing chamber connects to the bottom of the still in the same manner as the CFT's above the dilution unit (see Sec. 4.1.1). Sections are cut out of the tube so that a vacuum may also thermally isolate the heat exchangers.

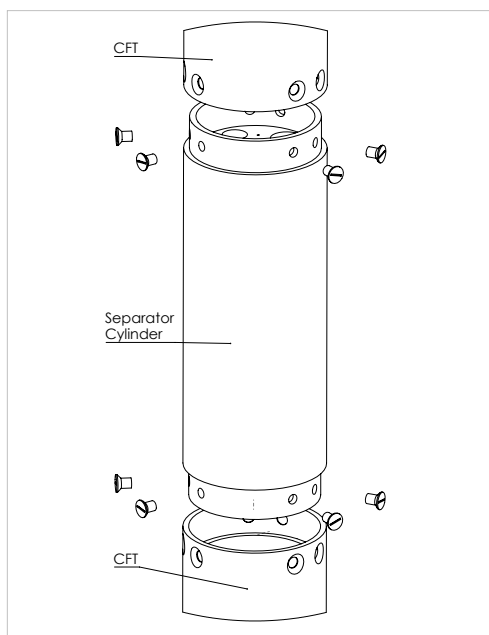


**Fig. 5** View of the CFT's fitting to the separator cylinder (inner piping is hidden for clarity).

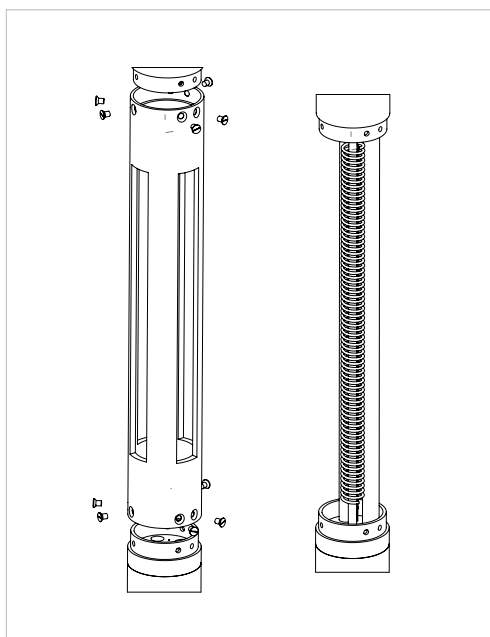


**Fig. 6** View of the region between the separator cylinder and the 1 K plate, with and without the CFT (left and right, respectively). In the left image, the open channels of the CFT may be seen. This is to allow 1 K  $^4\text{He}$  from the evaporator to cool the inner tubing. In the right image, a spiraling  $^3\text{He}$  in line is shown. This increase in tube length helps pre-cool and condense the incoming  $^3\text{He}$ .

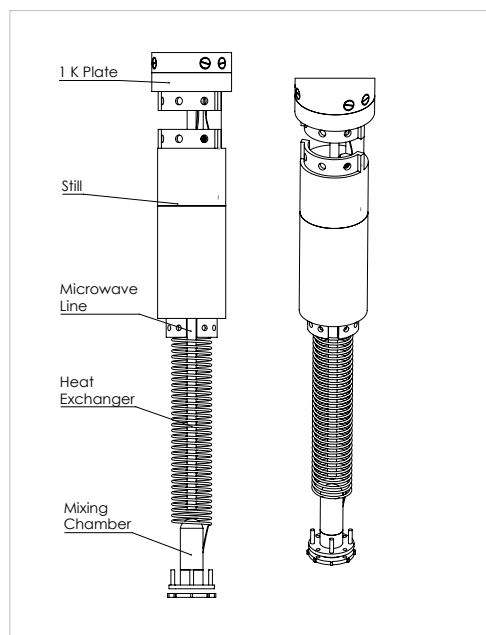


**Fig. 7** Dilution unit of the proposed insert. Shown are the 1 K Plate, the graphite connection between the 1 K and the still, the main heat exchangers, and the mixing chamber.

A vacuum jacket fits around the inner components of the refrigerator, making no direct contact. The design of this jacket is described in Sec. 4.2.1. Inside the vacuum jacket a vacuum is maintained to thermally isolate the low temperature inner components of the refrigerator, preventing heat leaks from affecting performance. This vacuum is established by the vacuum line that runs down from the upper flange and terminates at the 1 K plate (see Fig. 9).

A graphite support connects the still to the 1 K plate, while the main graphite support connects the still to the mixing chamber. The main heat exchanger is a tube-in-tube, counter-current continuous heat exchanger, the design of which is discussed in Sec. 4.2.6. The microwave line and NMR line penetrates the 1 K plate and still, and travels down toward the mixing chamber. Direct contact between the NMR line and the mixing chamber is prevented by having a crystal-glass window atop the mixing chamber, allowing the microwaves and NMR-RF to pass through to the sample inside the mixing chamber, the coldest part of the refrigerator. This crystal-glass window and mixing chamber geometry is described in Sec. 4.2.7. From the top of the 1 K plate to the bottom of the vacuum jacket, the dilution unit is 26.3 cm in length with a diameter of 4.22 cm (including the vacuum jacket).

#### 4.2.1 Vacuum Jacket

The vacuum jacket that encases the components of the dilution unit is stainless steel, and is comprised of two parts. The first is noted as the main jacket, attached at

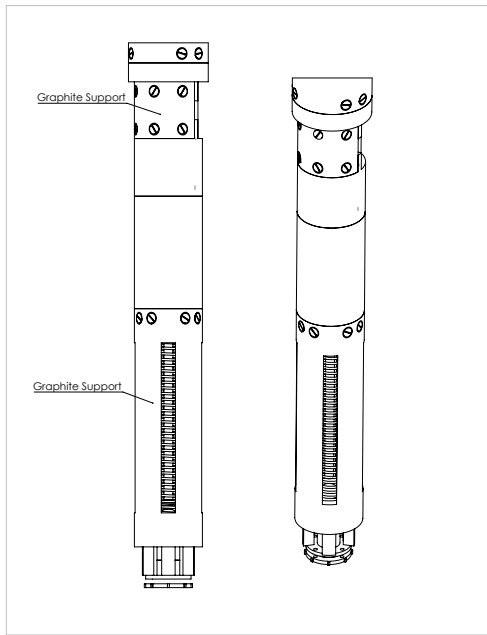


**Fig. 8** Dilution unit of the proposed insert, including the graphite support between still and mixing chamber.

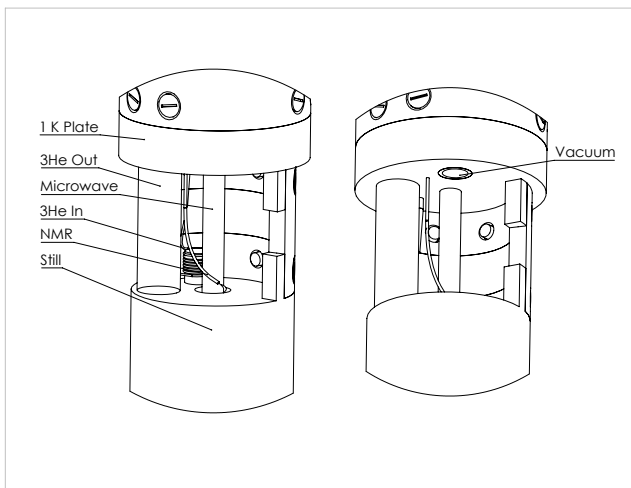


**Fig. 9** View of the area between the 1 K plate and the still.

the 1 K plate and surrounding all of the components (see Fig. 10). It is 0.6 mm in thickness (enough to withstand a 2 atm pressure differential without buckling) and is separated from the inner components by at least 2.5 mm at any point along its height.

The second is the vacuum jacket cap at the bottom of the dilution unit. While the main jacket is attached to the 1 K plate, the vacuum jacket cap is completely detachable, allowing easy access to the mixing chamber when load/unloading samples.

Where the cap attaches to the main jacket, both have a divot for the indium seal as well as a number of 2 mm screws holes. The indium provides a hermetic seal be-

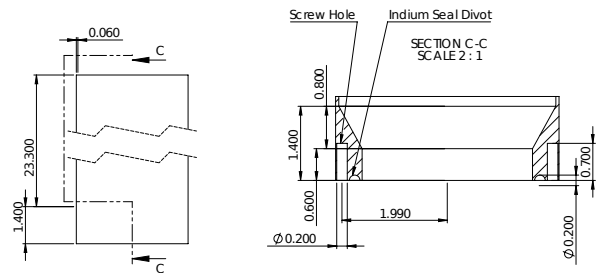


**Fig. 10** Main vacuum jacket, surrounding the inner components of the dilution refrigerator.

tween the two parts, supporting the high-vacuum environment within the vacuum jacket.

#### 4.2.2 Pre-cooler/Condenser & Main Impedance

As mentioned before, the incoming  $^3\text{He}$  runs through about 2.5 m of tubing held at 1 K in order to pre-cool/condense the  $^3\text{He}$  as it approaches the dilution unit (Sec. 4.1.2). In order for  $^3\text{He}$  to condense, the gas must be held at a high-enough pressure. For a pre-cooler held at about 1 K,  $^3\text{He}$  can condense in a pressure range of 25-200 torr [5]. The main impedance immediately follows the pre-cooler on the  $^3\text{He}$  in line, and is required for both creating the pressure needed to condense and controlling the molar flow rate. The molar flow rate (the rate at which liquid  $^3\text{He}$  leaves the condenser) must be less than the rate at which the system condenses for functioning continuous circulation [6].

The  $^3\text{He}$  travels through the series of heat exchangers in which the  $^3\text{He}$  is cooled by the dilute phase. These are common tube-in-tube continuous counter-current heat exchangers. Construction simply consists of fitting one smaller tube inside of a larger tube. Liquid  $^3\text{He}$  is sent downward through the inner tube while the cooler dilute phase fills the outer tube space. This heat exchanger is immediately after the still. To see this, consider Eq. 1 for  $n_3$  moles that pass through the phase boundary, the amount of heat that is absorbed is equal to the difference in the molar enthalpy of  $^3\text{He}$  in the dilute phase, or  $H_d(T)$ , and the molar enthalpy of  $^3\text{He}$  in the concentrated phase, or  $H_c(T)$ , both of which are functions of temperature  $T$ . The rate of heat absorption, or cooling power, then can easily be formulated to be:

$$\dot{Q} = n_3(96T_M^2 - 12T_N^2). \quad (1)$$

In the case of no cooling power, or  $\dot{Q} = 0$ , the condition for *any* cooling to take place is  $T_N/T_M \leq 3$ . This stresses the importance of proper heat exchange, as a dilution refrigerator whose mixing chamber has a temperature 50 mK must cool its incoming  $^3\text{He}$  from 0.7 K down to at least 150 mK for cooling to happen.

Exiting the series of heat exchangers above,  $^3\text{He}$  then enters into the mixing chamber. Here, the incoming  $^3\text{He}$

is sent to the concentrated phase, sitting atop the dilute phase. By an osmotic pressure gradient created at the still,  $^3\text{He}$  in the dilute side is moved away from the phase boundary. This in turn lowers the local binding energy of the dilute phase at the phase boundary, inviting more  $^3\text{He}$  atoms to leave the concentrated phase and transition into the dilute phase, producing the desired dilution cooling.

#### 4.2.3 Still

The still is a simple stainless steel cylinder that interfaces with the  $^3\text{He}$  pump-out and serves as a reservoir for the dilute-phase towards which the circulating  $^3\text{He}$  travels. The pre-cooled  $^3\text{He}$  comes into the still in a separate isolated line which passes through a thin tube continuous heat exchanger immersed in the liquid of the still. This  $\text{He}^3$  heat exchanger is made [7] of cupronickel tubing of 0.4 mm OD and 0.08 thickness, with a total length of 150 cm submerged in the liquid. This length of tubing can be easily contained within the still space. During operation the still would be held at about 0.7 K. The length of the submerged tube is chosen so that the  $^3\text{He}$  can cool to this temperature.

The  $^3\text{He}$  should then leave the still and move into a secondary impedance to maintain a suitable pressure in the still to retard the  $^3\text{He}$  evaporation. Under normal dilution operation osmotic pressure pushes the  $^3\text{He}$  from the mixing chamber, through the heat exchangers and eventually back to the still. When the mixture is optimized and the still holds the minimal required volume of liquid the  $^3\text{He}$  rests in the dilute phase.

The entire volume of the still is not dedicated to the dilute phase as the volume also contains  $^3\text{He}/^4\text{He}$  vapor and the liquid level should remain below the film-suppressor. Connected to the top of the still is a tube that leads directly outside the refrigerator to the sealed  $^3\text{He}$  pump system used to remove the  $^3\text{He}/^4\text{He}$  vapor. As more  $^3\text{He}$  turns back into vapor, less is left in the dilute phase at the vapor-liquid boundary. This difference in  $^3\text{He}$  concentration from the mixing chamber to the still is what creates the osmotic pressure difference that drives the  $^3\text{He}$  throughout the entire dilute phase.

The vapor pressure must be high enough to allow a reasonable flow rate of  $^3\text{He}$  through the refrigerator, which is achieved at temperatures higher than what the still naturally settles to in steady-state operation. For this reason a still heater is used to generate greater vapor pressure. The still heater will be a set of heating coils fixed inside the still. Increasing the temperature in the still also increases the partial pressure of  $^4\text{He}$ . In practice, it is beneficial to the performance of the dilution refrigerator to reduce the amount of  $^4\text{He}$  circulating with the  $^3\text{He}$  to minimize the temperature gradient instabilities, as well as the heat load to the heat exchangers. The challenge, then, is to heat the still to a temperature leading to an optimized total pressure while at the same time min-

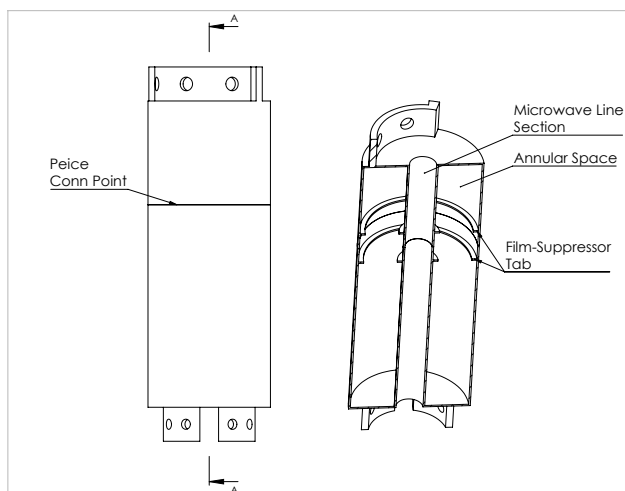


**Fig. 11** Cross-section of the still, showing the section for the microwave line and the annular space for the dilute liquid. Also shown are the tabs on which the film suppressors are supported within the still, as well as the location of the connection between the two still pieces.

imizing the partial pressure of the  $^4\text{He}$ . Generally this temperature has been found to be the aforementioned  $\sim 0.7$  K [8].

In this design of the still there is a hollowed space down the center of the cylinder, creating an annular space for the dilute  $^3\text{He}$  (Fig. 11). This allows the microwave and NMR line to run down to the mixing chamber without having to pass in through the still. The still has an OD of 3.6 cm, and inner diameter ID of 8 mm, with 0.5 mm thick walls. Both the  $^3\text{He}$  out-line and the  $^3\text{He}$  in-line are connected to the annular space of the cylinder through the top of the still (see Fig. 9).

In designing the still we keep two main points in mind [9]. First, the free surface area of the liquid on the dilute side must be large enough to facilitate an appropriate amount of evaporation. This is especially concerning if the free surface area is not something controllable due to the size constraints. Given a liquid surface of 4 cm in diameter, the resulting surface area would then be  $13 \text{ cm}^2$  leading to a molar flow rate greater than  $10^{-4}$  moles/sec. Secondly, the still must also prevent the circulation of  $^4\text{He}$ , which tends to crawl up the surfaces of the container in the form of a super-fluid film. This is prevented by the inclusion of a super-fluid film suppressor (see Fig. 11), which is simply a sharp edge over which the superfluid cannot travel. Two sharp edges must be included, since the annular space in which the dilute side sits has two inner surfaces.

#### 4.2.4 Secondary Impedance

As the  $^3\text{He}$  passes through the heat exchangers within the still, the pressure at which it passes should remain considerably above vapor pressure, lest any  $^3\text{He}$  re-evaporate and add a greater heat load to the system. To avoid this,

it is common practice to add a secondary impedance immediately below the still, allowing pressure in the still to remain above vapor pressure. It is important to place the secondary impedance in the highest possible temperature ranges to prevent any viscous heating affects.

The pressure drop across the impedance itself should be low, to lessen any heating affects due to the isenthalpic expansion of the liquid  $^3\text{He}$ . This rise in temperature is approximately proportional to the molar volume of the  $^3\text{He}$  and inversely proportional to the molar specific heat:  $(\partial T/\partial P)_H \approx -v_3/c_p = -1.3 \text{ mK/torr}$  at 0.7K [6]. This value increases substantially the lower the temperature. With a pressure drop of around 10 torr, this conservatively allows the temperature in the still to be as high as 1 K before re-evaporation occurs, while raising the temperature of the concentrated phase an approximate 13 mK.

To create this impedance a short length of bare manganin wire can be inserted into the  $^3\text{He}$ -carrying cupronickel tubing restricting the line. Before final assembly, the impedance value can be tested and adjusted to allow for the desired pressure drop for the correct molar flow rate.

#### 4.2.5 Main Graphite Support

Connecting the still and the mixing chamber is a tube of length 12.6 cm with 3.6 cm OD and 2.75 cm ID. This tube fits around the bottom of the still and attaches via eight M3 machine screws. This design of the support provides stability and low thermal contact as it both secures the mixing chamber and allows room for the NMR and microwave line at the center of the unit.

The material chosen for this main support is pitch-bonded graphite [10]. This type of graphite is uniquely useful for our purposes as it is a good thermal conductor at higher (room) temperatures and becomes a poor thermal conductor at lower (cryogenic) temperatures, i.e. it acts as passive heat switch. This allows quick-cooling when the dilution process first begins and the innards are still room temperature, and prevents a big heat load to the mixing chamber during steady-state operation.

#### 4.2.6 Heat Exchangers

The main heat exchanger of the proposed dilution insert is a tube-in-tube, counter-current continuous heat exchanger 200 cm in length and comprised of a 70% copper and 30% nickel alloy. The outer tube has an OD of 1.19 mm and ID of 1.03 mm, while the inner tube has an OD of 0.4 mm and ID of 0.24 mm. This style of heat exchanger is both very effective and compact. Despite a length of 200 cm, a coiling of 2 cm diameter with adequate spacing in between each coil reduces this length into about 10 cm in height, which may easily fit into the insert.

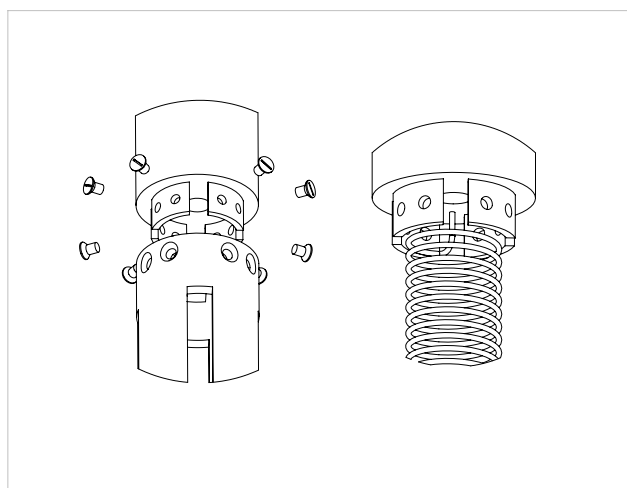


**Fig. 12** View of the area below the still. The image on the left shows how the main graphite support connects to the bottom of the still, while the image to the right the main heat exchanger spiraling down to the mixing chamber (graphite support hidden).

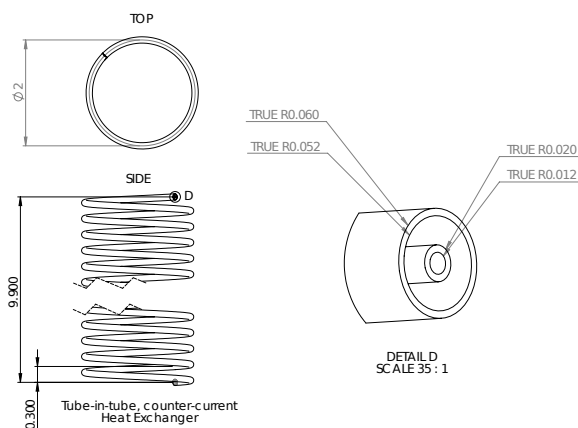


**Fig. 13** Main heat exchanger for the proposed dilution unit.

#### 4.2.7 Mixing Chamber

The mixing chamber is made of 1.8 mm crystal-glass wall which is sealed to a copper housing using a low temperature epoxy. As mentioned before, the crystal-glass window is used so that the NMR RF and the microwaves for DNP can pass through. The mixing chamber is secured to the graphite support via fitted pegs that are wedged into peg holes. Fig. 14 shows both the pegs on the mixing chamber as well as the peg holes of the graphite support. In this figure one can see the copper mixing chamber as well as the crystal-glass window and the peg holds located on the graphite support. This design for the mixing chamber has an inner volume of  $1 \text{ cm}^3$ .

Similar to the cap of the vacuum jacket, the mixing chamber cap has a groove an indium seal, as well as 2



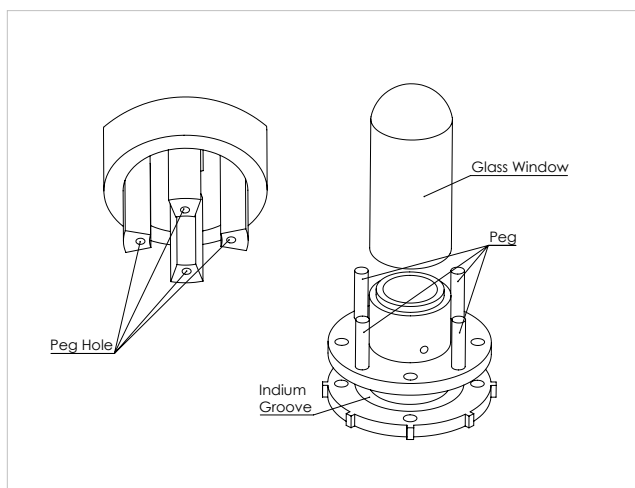


**Fig. 14** View of the mixing chamber (right) as well as the peg holds located on the graphite support (left). The mixing chamber will be made of copper and have an inner volume of about  $1 \text{ cm}^3$ .

mm screw holes. Samples are loaded and unloaded by removing this cap, accessing inside the mixing chamber. It is desired that the torque from screwing (unscrewing) these screws in the mixing chamber cap won't damage the graphite support to which it is attached. Our design allows for the insert itself to be secured upside-down, so that the mixing chamber is toward the ceiling while the cap is placed in a special "keyed" table so when torque is applied to tighten (loosen) the screws, that torque will be transferred to the table, and not the insert. In Fig. 14 this key is shown in the form of small tabs on the cap, that would fit into a supporting table for assembly (disassembly). Shown in Fig. 15 is the full dilution unit and the support structure that holds the mixing chamber.

## 5 Design Analysis

In designing the dilution insert, it is prudent to consider several different factors that are essential to operation: the heat load of the mixing chamber, heat exchanger analysis, and the pressure profile for the circulating  $^3\text{He}$ . While some design parameters are adjustable, these specifically must be well understood to confirm the functionality, and aid in the realization, of the dilution unit.

### 5.1 Heat Load of the Mixing Chamber

The heat load of the mixing chamber is extremely important to the operation of the dilution unit, as it is one of the factors that determine the minimum temperature achievable. This heat load comes in three different varieties. First, the mixing chamber must be initially cooled down from room temperature to 1 K, the temperature of

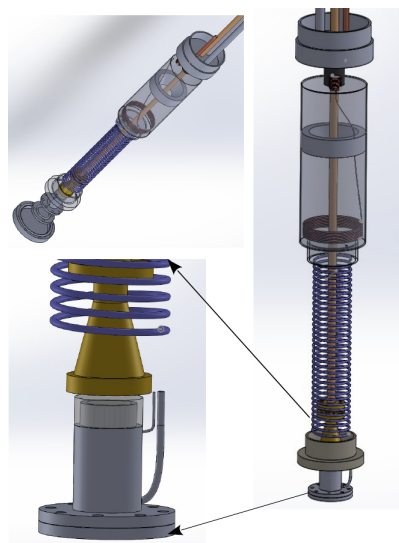


**Fig. 15** Full dilution unit and the support structure that hold the mixing chamber as well as the main heat exchanger.

the surrounding liquid Helium. Since the mixing chamber will initially contain a sample that needs to be kept at cryogenic temperatures, Sec. 5.1.1 is thus concerned with how much estimated time is needed to cool down the metal of the mixing chamber. Sec. 5.1.2 looks at expected heat leaks to the mixing chamber during regular operation of the dilution refrigerator.

#### 5.1.1 Initial Heat Load

When the dilution unit is first inserted into the cryostat, the components of the refrigerator are first cooled down by the surrounding 1 K  $^4\text{He}$  liquid. More specifically, heat is transferred from the innards of the dilution unit towards the 1 K plate and into the surrounding  $^4\text{He}$  being pumped on. An approximation of the time needed for this initial cooldown is important since the sample placed within the mixing chamber must remain at cryogenic temperatures. The samples used in solid polarized DNP experiments are usually stored in liquid nitrogen. For the preservation of the paramagnetic centers it's necessary to keep this material under 120 K at all times. The inner parts of the dilution unit must cool at such a rate so that the mixing chamber stays below this once the sample is loaded.

A simulation was developed to predict an approximate cooldown time. The innards of the refrigerator were treated as a one-dimensional bar with several sections of differing material, corresponding to the different components of the refrigerator. A summary of the simulated parts in order from top to bottom is as follows: 1 K plate (aluminum, 1 cm), graphite support (pitch-bonded graphite, 1.5 cm), still (aluminum, 9 cm), main graphite support (pitch-bonded graphite, 12 cm) and mixing chamber (copper, 3.2 cm). The simulated 1D

bar was comprised of these subsections, spatially ordered as they were listed, with a total length of 26.7 cm.

The 1D heat equation is used to determine how heat is dynamically transferred. The temperature  $T$  of the 1D bar is determined by the thermal conductance  $k$ , density  $\rho$  and specific heat  $c$ , such that,

$$\rho c \frac{\partial T}{\partial t} = k \frac{\partial^2 T}{\partial x^2} + \frac{dk}{dT} \left( \frac{\partial T}{\partial x} \right)^2. \quad (2)$$

Numerically solutions to Eq. 2 were generated over both time and space for given starting and boundary conditions. Information was obtained on thermal conductivity, heat capacity and density for copper, aluminum and pitch-bonded graphite to help accurately model the thermal properties of the bar [11] [12] [13] [14] [15] [16]. The entire bar was initially set to a temperature of 300 K with one end in contact with a reservoir of temperature 1 K representing the point at which the 1 K plate touches the 1 K  $^4\text{He}$ .

Fig. 16 shows the temperature profile of the dilution innards after ten minutes of cooling. One prominent feature that may be noted is that the refrigerator begins cooling very quickly after first contact. Within four minutes the mixing chamber cools below 200 K. The 1 K plate cools very quickly, becoming 1 K almost immediately. The rest of the refrigerator fails to cool this quickly due to the graphite support between the 1 K plate and the still, and prevents these lower components from cooling more than approximately 90 K, even after several hours. The reason for this is due to the graphite support acting as a passive heat switch for the refrigerator. The simulation highlights the fact that when the graphite support connecting the 1 K plate and the still reaches a certain low temperature during the cooldown, further cooling is halted due to this specific feature. For the purposes of thermally isolating the mixing chamber this is very good. But in the interest of preventing this slowing down of the cooling the inner vacuum space can be pressurize with helium gas. This exchange gas at about 40 mbar can be used to more quickly ( $\sim 30$  min.) bring the temperature down by thermally connecting the 1 K plate with the dilution components. After cooling the exchange gas must then be pumped out to re-establish the insulating vacuum. Fortunately, the simulation indicate that passive cooling alone is enough to keep the sample undamaged. In practice, there should be several minutes where the material in the mixing chamber is accompanied by liquid nitrogen, to give time for re-assembly and cooldown initialization.

### 5.1.2 Continuous Heat Leak

During continuous operation, heat leaks to the mixing chamber balance the cooling capacity of the refrigerator as it reaches its minimum temperature. The inner vacuum surrounding the dilution unit is designed to thermally isolate the low temperature components so that

the main heat leak present during continuous operation is the heat transferred through the main graphite support. Using recent data on pitch-bonded graphite [15], the tube with dimensions given in Sec. 4.2.5 would transmit approximately 25 nW of heat from a 0.7 K still to a 50 mK mixing chamber. This kind of heat load is more than manageable for the proposed refrigerator (see next section).

## 5.2 Heat Exchanger Analysis

Much analysis has been done on continuous heat exchangers, both numerically and experimentally. A “good” continuous heat exchanger [6] is one in which the heat transferred along the heat exchanger is small compared to the total heat transferred. In quantitative terms, a ratio can be defined in terms of the thermal conductance  $\kappa$ , cross-sectional area  $A$ , total length  $L$ , molar flow rate  $\dot{n}_3$  and molar specific heat  $c$ :

$$Y_i = \frac{\kappa_i A_i}{L_i \dot{n}_3 c_j}. \quad (3)$$

The subscript  $i$  may be  $c$ ,  $d$  or  $b$ , representing the column of liquid  $^3\text{He}$  contained within the inner tube, the column of dilute  $^4\text{He}$  in the annular space, and the body of the heat exchanger itself.

The total  $Y$  is the sum of these three ratios, and in order to be a suitable heat exchanger must be small in magnitude:

$$Y = \sum_i Y_i = \sum_i \frac{\kappa_i A_i}{L_i \dot{n}_3 c_j} \ll 1. \quad (4)$$

Once this is determined it is also possible to find the resulting temperature gradient along the heat exchanger [6]. Given an infinitesimal length of exchanger  $dx$ , there will be three main avenues of heat transfer: heat conduction along the heat exchanger by the established temperature gradient between the still and mixing chamber, Kapitza conduction between the dilute phase and concentrated phase, and viscous heat effects. All three of these contribute to the total change in enthalpy occurring in each section of the heat exchanger.

For a continuous heat exchanger that, in addition to the features above, also has a surface area of  $\sigma$  between the dilute and concentrated phase, a Kapitza resistance of  $\rho(T)$ , and a temperature of  $T_b$  with the liquid it carries having a viscosity  $\eta$ , molar volume  $v_3$ , and flow impedance  $z$ , the following coupled differential equation then gives the temperature of either the dilute or concentrated side as:

$$\underbrace{\dot{n}_3 c_i \frac{dT_i}{dx}}_{\text{Enthalpy change}} = A_i \underbrace{\left[ \kappa_i \frac{d^2 T_i}{dx^2} + \frac{d\kappa_i}{dT_i} \left( \frac{dT_i}{dx} \right)^2 \right]}_{\text{Heat conduction}}$$

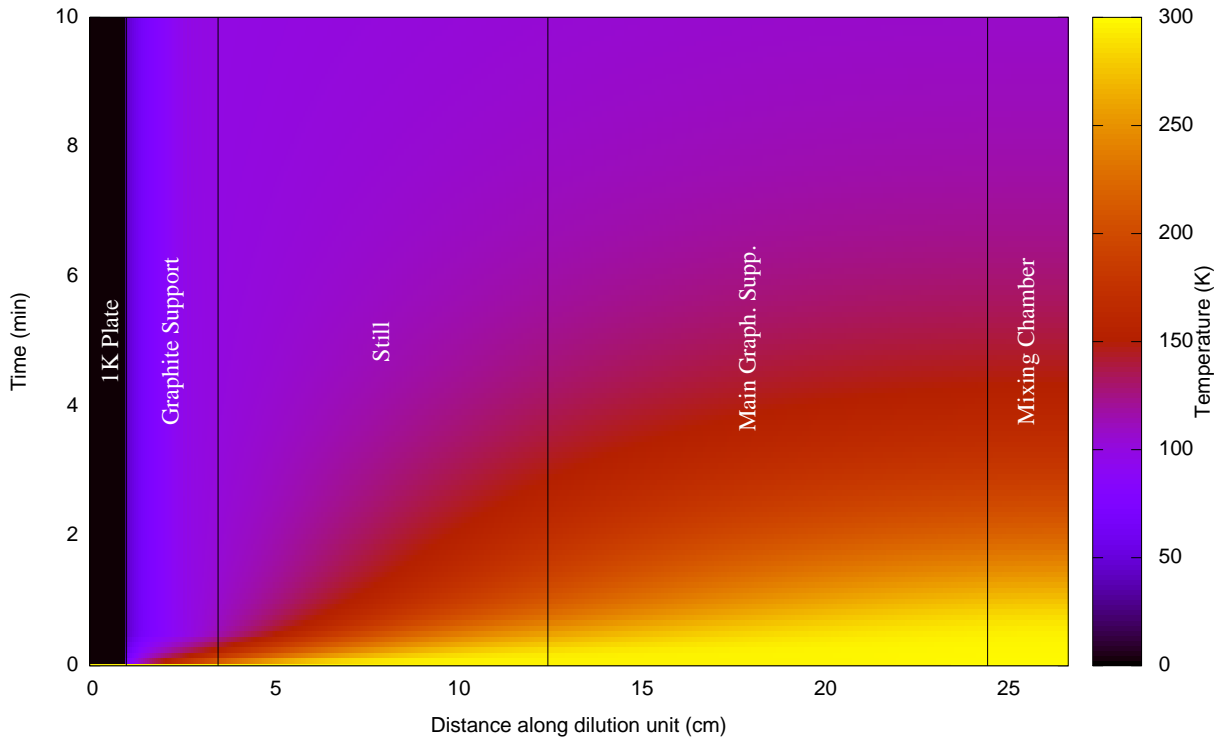


**Fig. 16** Temperature profile of the dilution refrigerator innards after ten minutes of cooldown. Each portion of the dilution unit is marked on the figure.

$$- \underbrace{\frac{d\sigma_i}{dx} \int_{T_b}^{T_i} \frac{dT}{\rho_i}}_{\text{Kaptiza conduction}} + \underbrace{\eta v_3^2 n_3^2 \frac{dz}{dx}}_{\text{Viscous Heating}}.$$

In Sec. 4.2.6 we detail our continuous heat exchanger for this system. With only about a meter of this type of heat exchanger, a dilution refrigerator could potentially be able to obtain a low temperature of 26 mK [7]. The cupronickel tubing made of 70% copper and 30% nickel, has a significantly lower thermal conductivity than other alloys, or even other cupronickel alloys. However, research has only been done on the transport properties of cupronickel material down to 4K, nowhere near the range desired. This 4 K conductance can still be taken as the *upper limit* on the actual conductance, as thermal conductance generally falls with decreasing temperature. Thus, we use  $\kappa_b \leq 0.0072$  (W/cm K) [17].

As for the  $c_b$ , this value should be best given as the molar heat capacity of the dilute side [6], which has an upper limit of approximately  $75 \text{ J mol}^{-1} \text{ K}^{-1}$ .

Together, these values result in a maximum value for  $Y_b$  to be 0.005. This satisfies the condition placed by Eq. 4, meaning that this particular heat exchanger is ideal. The term in Eq. 5 due to heat conduction can then be ignored.

The Kaptiza resistance of the concentrated side for temperatures between .7K and .13K can be approximated as [18] :

$$\rho_c(T_c) = \left( \frac{2.4}{T_c^4} + \frac{1.55}{T_c^3} \right) \times 10^{-5} \quad (5)$$

While at temperatures between .01 K and .13K, the following approximation is more appropriate:

$$\rho_c(T_c) = \left( \frac{20}{T_c^3} \right) \times 10^{-5} \quad (6)$$

For the dilute side, its Kaptiza resistivity can be approximated over the entire temperature range with:

$$\rho_d(T_d) = \left( \frac{7}{T_d^3} \right) \times 10^{-5} \quad (7)$$

Ignoring any viscous heating affects, all change in enthalpy, then, would be the cause of the Kapitza conduction; any heat leaving the concentrated side would (ideally) go directly into the dilute side such that [18],

$$\frac{d\sigma_c}{dx} \int_{T_b}^{T_c} \frac{dT}{\rho_c} = \frac{d\sigma_d}{dx} \int_{T_d}^{T_b} \frac{dT}{\rho_d}. \quad (8)$$

This integral can be solved numerically for  $T_b$  in terms of  $T_c$  and  $T_d$ , given the Kaptiza conduction values for the concentrated and dilute side.

The value of  $\frac{d\sigma_i}{dx}$  for Wheatley's heat exchanger is simply  $2\pi r_i$ , where  $r_i$  is the radius of the inner tube that touches either the concentrated side ( $r_c = 0.32$  mm) or the dilute side ( $r_d = 0.4$  mm).

Simplifying Eq. 5 by ignoring the heat conduction and viscous heating terms, one can rearrange and reduce the expression to find the change in temperature per unit length:

$$\frac{dT_i}{dx} = -\frac{2\pi r_i}{\dot{n}_3 c_i} \int_{T_b}^{T_i} \frac{dT}{\rho_i} \quad (9)$$

A simple program was made to analyze heat exchanger lengths and heat loads. Taking as input the desired mixing chamber temperature, heat load and molar flow rate, Eq. 1 was used to find the temperature on the concentrated side necessary to match those conditions. These two temperatures  $T_{mc}$  and  $T_c$ , for the dilute and concentrated side respectively, were the starting point for the analysis. From these values, Eq. 9 could be used by iteration to create a profile of the temperature as a function of distance from the mixing chamber.

Fig. 17 shows the resulting temperature profiles for several of these simulations. Keeping the flow rate of  $^3\text{He}$  at a constant  $10^{-4}$  mol/s across all simulations, mixing chamber temperatures of 100 mK down to 50 mK (as labeled on the graph) were tested against a heat load of  $\dot{Q} = 10^{-9}$  and  $10^{-6}$  W.

Looking at Fig. 17, it is apparent how the Kapitza resistance becomes more of an issue at lower desired mixing chamber temperatures. For a heat load of  $10^{-6}$  W, a mere 25 cm of continuous heat exchanger is needed to reach 100 mK, while the same heat load requires nearly 2 meters for 50 mK. This could potentially achieved a minimum mixing chamber temperature of 26 mK with a molar flow rate of  $10^{-5}$  mol/s [7].

Fig. 17 also suggests that a heat load of  $10^{-6}$  W or below is more than manageable for a heat exchanger of length 200 cm. Variations in heat load in this range also do not wildly impact the length of exchanger needed. For example, for a mixing chamber of 50 mK, an increase of heat load from  $10^{-9}$  W to  $10^{-6}$  W only requires a 10 cm extension of heat exchanger. Higher heat loads, however, become tricky. The reason for this is due to the limitations on the cooling power for a given molar flow rate. This can be seen by rearranging the change in enthalpy that occurs at the phase boundary Eq.1, finding instead the temperature of the incoming  $^3\text{He}$  as a function of cooling power:

$$T_N = \sqrt{\frac{1}{12} \left( 96T_M^2 - \frac{\dot{Q}}{\dot{n}_3} \right)}. \quad (10)$$

The value of  $T_N$  should be real so the sign under the radical should remain positive implying that there is a point at which it is physically impossible to obtain a desired mixing chamber temperature for a given heat load. For a molar flow rate of  $10^{-4}$  mol/s and desired

mixing chamber temperatures under 100 mK, this heat load starts to occur around tens of microWatts. Eq.10 suggests that the only solution to a higher heat load is an increase in the circulation of  $^3\text{He}$ . This comes at a price, however, as the rate of temperature change along the heat exchanger, Eq.9, is lowered by the raising of molar flow rate. Indeed, the effects are not trivial: for a heat load of 1 microWatt and a desired mixing chamber temperature of 100 mK, a flow rate of  $10^{-3}$  mol/s would need about 250 cm of heat exchanger - nearly ten times the length needed with a flow rate of  $10^{-4}$  mol/s. The strategy, then, should be to determine the minimum flow rate needed to achieve a desired mixing chamber temperature for the expected heat load, as this would also help determine the minimum length of heat exchanger needed.

This concern is not too prevalent in our design, as 100 nW of heat to the mixing chamber (while the microwave beam is turned off) is itself a very conservative estimation. Nonetheless, it is good to keep these things in mind for any future experimentation of the cooling power of the dilution unit.

### 5.3 Pressure Profile

Given that the pressure of the concentrated side is important to several points in the dilution refrigerator, it is prudent to consider the pressure and/or pressure drop at each point in the journey of the  $\text{He}^3$ .

#### 5.3.1 Pressure Gradient Along a Circular Heat Exchanger

Consider a pipe of diameter  $D$  (cm) and length  $L$  (cm), through which a fluid of molar mass  $M$  (g/mol), density  $\rho$  (g/cm $^{-3}$ ) and viscosity  $\eta$  (poise) flows at a molar flow rate of  $\dot{n}$ . The pressure drop  $\Delta P$  that occurs due to viscous effects in the liquid as it travels across the length of the pipe is then given by the Darcy-Weisbach equation [19]:

$$\Delta P = \frac{1}{2} \psi \frac{LG^2}{D\rho}. \quad (11)$$

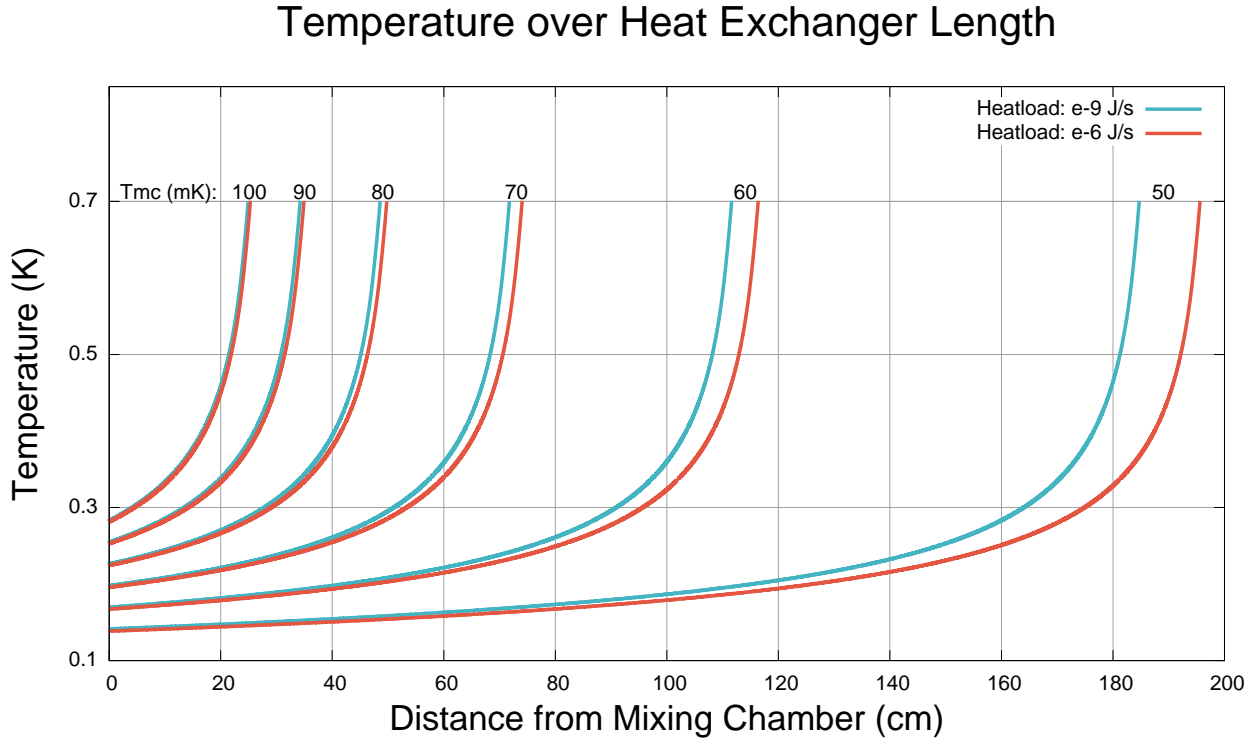
Here, we define  $G$  as:

$$G = \frac{M\dot{n}}{\pi D^2}, \quad (12)$$

and  $\psi$  is a dimensionless factor called the *Darcy Friction Factor*, and is dependent on the physical situation within the pipe, such as the shape and material of the pipe, as well as characteristics of the material flowing through it. It is usually dependent on the Reynolds number  $RE$  of the enclosed fluid (also dimensionless) given as,

$$RE = \frac{GD}{\eta}. \quad (13)$$

Fig. 17 Temperature profile for several different heat exchanger situations.



A Reynolds number of value less than 2300 corresponds to a regime of fluid flow (*laminar flow*), while RE values above this mark are considered to have *turbulent* flow [19]. Laminar flow is characterized as high momentum diffusion and low momentum convection, i.e. the fluid is more-or-less well behaved as it moves from one end of the tube to another. Turbulent flow, as the name suggests, occurs when the flowing fluid is more sporadic and chaotic in nature, with a low momentum diffusion and high momentum convection. For a circular pipe in the laminar flow regime, the Darcy Friction Factor is:

$$\psi_{lam} = \frac{64}{RE}. \quad (14)$$

The Darcy Friction Factor for turbulent flow, on the other hand, is given [19] as:

$$\psi_{turb} = 0.316(RE)^{-0.25}. \quad (15)$$

### 5.3.2 Pertinent Properties of $^3\text{He}$

In order to use the above equations, it is necessary to determine some properties of liquid  $^3\text{He}$  as it travels towards the phase boundary; namely viscosity, molar mass and molar density. The viscosity of the concentrated side as a “limiting low-temperature” value is given by [10]:

$$\eta_c = (2 \times 10^{-6})/T^{-2}. \quad (16)$$

The molar mass of  $^3\text{He}$  is 3.02 g/mol, and its molar density can be approximated to be 0.08 g/cm $^{-3}$  for temperatures of under 1 K [20].

### 5.3.3 Tracing the Pressure Profile

At the phase boundary, zero pressure difference is wanted between the concentrated and dilute sides, since the phase boundary should sit within the mixing chamber. A numerical analysis is used, incorporating the above equations to estimate the pressure experienced by the  $^3\text{He}$  as it travels into the dilution unit and towards the mixing chamber. Care was taken to ensure pressures are high enough for the incoming  $^3\text{He}$  to condense as it approaches the 1 K plate, as well as stay condensed inside the still (provided by a main and secondary impedance; see Sec. 4.2.2 and 4.2.4). Table 5.3.3 shows this pressure profile in terms of the pressure and pressure difference as well as the impedance value at several location in the still, the mid location within primary and secondary impedance, the heat exchangers and the mixing chamber phase boundary. The phase boundary is non-zero as this is the pressure needed from the incoming  $^3\text{He}$  to counteract the pressure of the dilution mixture.

## 6 Conclusion

We have proposed a design for a dilution refrigerator insert to an existing Oxford cryostat to be used in experimental research. The system is designed to polarized materials using DNP and then to switch to a frozen-spin mode where the microwaves are turned off and the  $^3\text{He}$

Table 1. Pressure profile of incoming  $^3\text{He}$ 

Position	$P$ (torr)	$\Delta P$ (torr)	Imp. ( $\text{cm}^{-3}$ )
Overhead	50	—	—
Pri. Imp.	—	-38	$3.8^{11}$
Still, Upper	12	—	—
Still HE	—	(negligible)	$5.83^9$
Still, Low	12	—	—
Sec. Imp.	—	-10.87	$1.1^{11}$
HE, Upper	1.137	—	—
HE	—	-0.001	$1.94^{10}$
Phase Bou.	1.136	—	—

circulation begins. This new insert provides the flexibility to change the Oxford configuration from a high power evaporation refrigerator to a low temperature dilution refrigerator and back in a quick straight forward manner.

Borrowing from over fifty years of dilution refrigeration research, this compact design also attempts to maximize overall performance while remaining within the limiting geometric constraints. Two notable design aspects are the continuous heat exchanger that is compact yet reaches temperatures in our goal range, as well as the use of pitch-bonded graphite as a passive heat switch between temperature-sensitive components of the refrigerator.

The cooling power of the refrigerator is discussed, including potential sources of heat leak and heat load. Several numerical analyses are also provided to model the performance of the proposed design. The initial cooldown of the insert is simulated, ensuring that the samples inserted into the mixing chamber preserve their paramagnetic centers needed for DNP. Temperature profiles of the proposed heat exchanger were calculated for different heat loads and mixing chamber temperatures. The expected pressure profile of the dilution unit is also estimated. Our studies suggest that the design proposed can be use effectively as a frozen-spin system in a research or academic lab.

**Acknowledgements** The authors thank the senior members of the solid polarized target lab at the University of Virginia. This work was supported by DOE contract DE-FG02-96ER40950.

## References

- D.G. Crabb and W. Meyer, *Ann. Rev. Nucl. Part. Sci.* **47**:67-109 (1997)
- C.D. Keith, et al. *NIM A* **684** (2012) 2735
- G.R. Court, et al., *NIM A* **324** (1993) 433
- D. Keller, *Nucl. Instr. and Meth.* **A728** 133 (2013)
- E. Ambler and R. Hudson *Research of the National Bureau of Standards Vol. 56, No. 2* (1956)
- R. Radebaugh and J.D. Siegwarth *Cryogenics* **11** (1971)
- Wheatly, J.C., Rapp, R.E. and Johnson, R.T., *J. Low Temperature Physics* **4** (1971)
- D. S. Betts, *An Introduction to Millikevin Technology*, Cambridge University Press, New York (1989)
- G. Frossati, *Proc. 15<sup>th</sup> Int. Conf. on Low Temperature Physics*, J. de Physique, Colloque C-6, Suppl. no. 8, Grenoble, France, 23-29 (1978)
- J. C. Wheatly, O.E. Vilches, and W.R. Abel *Phys.* **4** (1968)
- G.K. White, and S.J. Collocott, *J. Phys. Chem. Ref. Data* **13** (1984)
- K. Mendelsohn, and H.M. Rosenberg, *Proc. of the Phys. Soc. Section A* **65**, 6 (1952)
- J.E. Jensen, W.A. Tuttle, R.B. Stewart, H. Brechna, A.G. Prodel, *Brookhaven National Laboratory Selected Cryogenic Data Notebook*, **1** (Brook Haven National Laboratory 1980)
- R.G. Sheppard, D.M. Mathes, D.J. Bray, *Properties and Characteristics of Graphite for Industrial Applications* (POCO Graphite 2001)
- A.L. Woodcraft, M. Barucci, P.R. Hastings, L. Lolli, V. Martelli, L. Risegari, G. Ventura, *Cryogenics* **49**, 5 (2009)
- J.G. Hust, *A Fine-Grained, Isotropic Graphite for use as NBS Thermophysical Property RM's from 5 to 2500 K*, (National Bureau of Standards 1984)
- C. Y. Ho, M. W. Ackerman, K. Y. Wu, S. G. Oh, T. N. Havill, *Journal of Physical and Chemical Ref. Data* **7**, 959 (1978)
- J.D. Siegwarth, and R. Radebaugh, *The Review of Scientific Instruments* **42**, 8 (1971)
- G.K. White *Experimental Techniques in Low-Temperature Physics*, Stonebridge Press, Bristol (1968)
- R.W.H. Webeler, D.C. Hammer, *Physics Letters*, **21**, 4 403 June 1966, 403-404